Biochemical and Biophysical Research Communications 456 (2015) 197–201

Contents lists available at ScienceDirect

Biochemical and Biophysical Research Communications

journal homepage: www.elsevier.com/locate/ybbrc

Structural insight into the assembly of human anti-HIV dynamin-like protein MxB/Mx2

Bo Xu [a,b,1], Jia Kong [a,b,1], Xin Wang [a,b], Wei Wei [b,c,d], Wei Xie [a,b,*], Xiao-Fang Yu [a,b,c,d,*]

[a] School of Life Sciences, Tianjin University, Tianjin 300072, China
[b] Collaborative Innovation Center of Chemical Science and Engineering, Tianjin 300072, China
[c] Department of Molecular Microbiology and Immunology, Johns Hopkins Bloomberg School of Public Health, Baltimore, MD, United States
[d] Institute of Virology and AIDS Research, First Hospital of Jilin University, 519 E Minzhu Ave, Changchun, Jilin Province 130061, China

ARTICLE INFO

Article history:
Received 8 November 2014
Available online 22 November 2014

Keywords:
MxB
Crystal structure
Stalk domain
Dynamin-like protein
Anti-HIV activity

ABSTRACT

Interferon (IFN) is a key component of the innate immune response to exogenous pathogens. Interferon increases the mRNA levels of interferon-stimulated genes (ISGs) in vivo, which is thought to account for its antiviral activity. Recent studies have indicated that human myxovirus resistance protein 2 (Mx2 or MxB), one of these ISGs, contributes to the inhibition of HIV-1 replication by interferon. MxB may bind to HIV-1 relatively late in the post-entry phase, and it leads to a reduced level of integrated viral DNA, thereby restricting HIV-1 infection. The N-terminal 91-aa domain of MxB and the assembly of MxB mediated by the Stalk domain have also been shown to be indispensible for MxB's anti-viral functions, but the mechanism involved has remained elusive. Here, we report the crystal structure (2.9 Å) of the human MxB Stalk domain. MxB Stalk shows one dimer in the asymmetric unit. Each monomer contains a four-helix bundle. Interestingly, analyses of MxB dimer interfaces show that the majority of residues involved in the interface are not conserved between MxB and MxA, contributing to the building of a more stable MxB dimer. MxA and MxB Stalk domains share 46.7% sequence identity, and the structure of the MxA Stalk domain and the overall structure of MxB Stalk have a similar conformation. Our results indicate that although human Mx proteins share common structural characteristics, their dimerization strategies are unique, contributing to their unique contributions to viral restriction.

1. Introduction

Like most mammals, humans carry two *myxovirus resistance* genes, *MX1* and *MX2*, which have arisen by gene duplication [1–3] and encode the interferon-inducible dynamin-like GTPases MxA and MxB [3–5]. Human MxA and MxB share 63% amino acid (aa) sequence identity and a similar domain architecture [6], including a G domain that hydrolyzes GTP to GDP; a hinge-like "bundle signaling element" (BSE) that connects the G domain to the elongated Stalk domain; and the Stalk domain, which is involved in self-assembly (Fig. 1A) [7]. Mice also have two Mx proteins, both of which exhibit antiviral activity against a wide range of viruses [1,8]. Human MxA also has been shown to suppress a wide range of pathogenic DNA and RNA viruses, such as influenza A virus and hepatitis B virus [9,10]. In contrast, human MxB does not suppress the tested viruses and appears to have lost its antiviral activity [11].

However, MxB has been identified as a novel inhibitor of human immunodeficiency virus type-1 (HIV-1) [12–14]. MxB can bind to the HIV-1 at a relatively late post-entry phase and leads to a reduced level of integrated viral DNA, thereby restricting HIV-1 infection. The function of the N-terminal 91-aa domain of MxB, the critical determinant of MxB's antiviral activity, has been extensively explored: A fusion protein that combines the N-terminal 91-aa domain of MxB with the G, BSE, and Stalk domains of MxA still has antiviral activity [15], and the N-terminal 91-aa domain of MxB can directly bind to the HIV-1 capsid in vitro and in vivo, requiring no cellular co-factors [16–18]. Furthermore, the N-terminal 91-aa domain of Mx2B recognizes the higher-order lattice of CA tubes instead of CA hexamer or monomers [16,17]. Several mutations in the HIV-1 viral capsid (CA) region of Gag can overcome Mx2-mediated suppression [13,18].

In addition to the N-terminal 91-aa domain of MxB, the assembly and oligomerization of MxB have also been shown to be indispensible for MxB's anti-viral functions [18]. As is true of most

* Corresponding authors at: School of Life Sciences, Tianjin University, 92 Weijin Road, Nankai District, Tianjin 300072, China. Fax: +86 22 27403906.
E-mail addresses: xiewei.xray@gmail.com (W. Xie), xfyu@tju.edu.cn (X.-F. Yu).
[1] These authors contributed equally to this work.

http://dx.doi.org/10.1016/j.bbrc.2014.11.058
0006-291X/

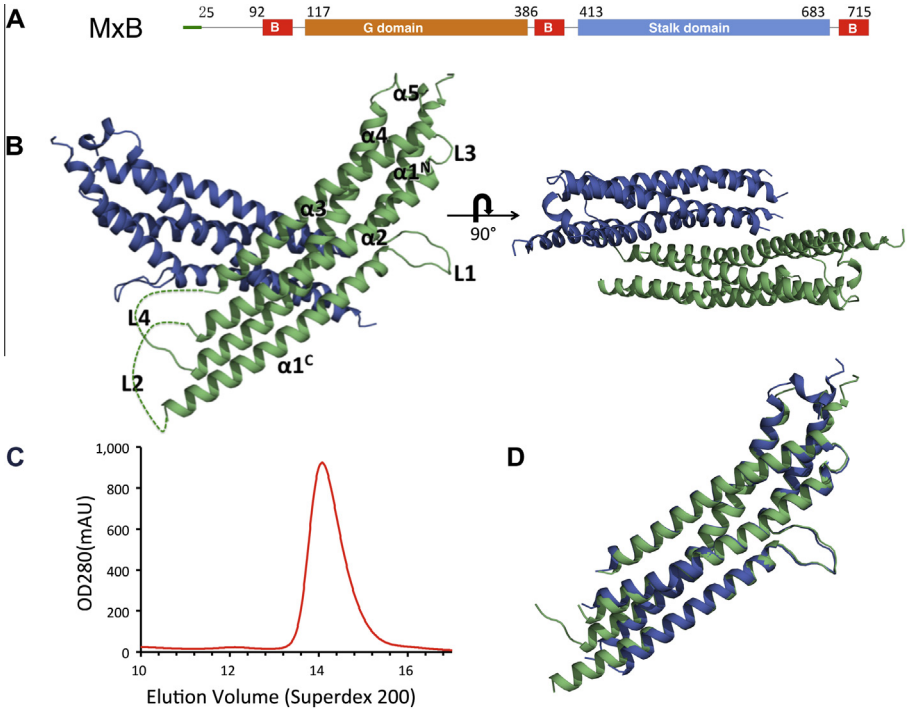

Fig. 1. Overall structure of the human MxB Stalk domain. (A) Structure-based domain representation of human MxB. The numbers of the amino acid residues at the boundaries of the domains are indicated. (B) Overall structure of the MxB Stalk domain in two perpendicular views. Monomers 1 and 2 are colored blue and green, respectively. (C) Gel-filtration profiles of the MxB Stalk domain. MxB Stalk (YRGK/AAAA) (red) elutes mainly in the dimer fraction. (D) Superposition of monomers 1 and 2. (For interpretation of the references to color in this figure legend, the reader is referred to the web version of this article.)

dynamin-like proteins, their cellular functions are assembly-stimulated, and it has been proposed that the assembly and oligomerization of MxB, mediated by the Stalk domain, may produce a higher binding affinity for the viral capsid, but the mechanism has remained elusive. MxA can assemble to form ring-like higher-order oligomers, but little is known about the assembly details of MxB. Here we report the crystal structure of the Stalk of human MxB and dissect its function in the assembly of MxB.

2. Materials and methods

2.1. Expression and purification of the MxB Stalk domain

The gene fragment encoding the MxB Stalk domain (413–683) was PCR-amplified from full-length MxB cDNA (XM_005260983) and cloned into the modified pQlink plasmid with an N-terminal His-tag. The mutations YRGK/AAAA and deletion loop L4 (580–607) were generated by site-directed mutagenesis and confirmed by custom sequencing analysis.

The proteins were over-expressed in *Escherichia coli* XL10 Gold cells. The cells were lysed using a French press in buffer containing 50 mM/L Tris–HCl at pH 8.0, 0.3 M/L NaCl, 10 mM/L imidazole, 1 mM/L PMSF, and 0.5% Triton X-100. The proteins were purified by Ni-NTA-affinity chromatography (GE Healthcare). The His-tag was cleaved by TEV protease and removed by Ni-NTA affinity chromatography. The proteins were sequentially purified on a Resource Q column and Superdex200 sizing column (GE Healthcare) in buffer (20 mM Tris–HCl, pH 8.0, with 150 mM NaCl and 0.5 mM TCEP).

2.2. Crystallization and X-ray data collection

The eluted fractions were analyzed by SDS–PAGE and concentrated to ~8 mg/mL for crystallization screening (Hampton Company). The crystals were optimized in 0.1 mol/L sodium acetate at pH 4.5 with 6% PEG 4000 by hanging-drop vapor diffusion at 18 °C and improved by the micro-seeding method. The diffraction of the crystals improved to 2.9 Å after dehydration in 0.1 mol/L sodium acetate at pH 4.5 with 15% PEG 4000 for approximately 0.5 h. The crystals were flash-frozen in liquid nitrogen before data collection [19]. The diffraction data sets were collected at the Shanghai Synchrotron Radiation Facility (SSRF) on beamline BL17U and processed with HKL2000 [20].

2.3. Structure determination and refinement

The crystal belonged to the P 31 2 1 space group, with one dimer of the Stalk domain per asymmetric unit. The structure was solved by molecular replacement using PHENIX [21,22], with the MxA Stalk structure (PDB ID: 3LJB) as the search model. Model building was performed with PHENIX [23] and modified with Coot [24], and refinement was carried out using PHENIX [25]. The final R_{work} and R_{free} values were 21.84% and 24.11%, respectively [26]. The final structure was analyzed with PROCHECK [27]. Data collection and refinement statistics are shown in Table 1. Associated structure figures were prepared using PyMol (http://www.pymol.org), and the coordinates were deposited in PDB under accession code 4X0R.

3. Results and discussion

3.1. Overall structure of the MxB Stalk domain

Despite rigorous trials, we were unable to obtain soluble full-length MxB protein for crystallization. After removal of the N-terminal 83aa, the expression level of MxB (84–715) was improved. To overcome the oligomerization, based on data from structural studies of MxA [7], we applied (YRGK487–490AAAA) and a deletion loop, L4, (580–607) to MxB (84–715). The majority of MxB

Table 1
Data collection and refinement statistics.

Wavelength (Å)	1.000
Resolution range (Å)	38.65–2.905 (3.009–2.905)
Space group	P 31 2 1
Unit cell	154.612 154.612 103.34 90 90 120
Unique reflections	31652 (3035)
Completeness (%)	99.77 (97.78)
Mean *I*/sigma(*I*)	18.74 (1.52)
Wilson *B*-factor	76.44
R-factor[a]	0.2184 (0.3168)
R-free[b]	0.2411 (0.3558)
Number of atoms	3491
Macromolecules	3491
Water	0
Protein residues	417
RMS(bonds)	0.009
RMS(angles)	1.24
Ramachandran favored (%)	97
Ramachandran outliers (%)	0
Clashscore	15.94
Average *B*-factor	104.70

Numbers in parentheses represent statistics for the highest resolution shell.
[a] $R_{work} = \sum||F_{obs}| - |F_{calc}||/\sum|F_{obs}|$.
[b] R_{free} = *R* factor for a selected subset (5%) of the reflections that were not included in prior refinement calculations.

(84–715) still behaved as an oligomerized form, but the Stalk domain (413–683), bearing the same mutations and deletion, yielded a monodispersed peak on a size-exclusion column (Fig. 1C). Crystals of the Stalk domain (413–683) of MxB, which diffracted to a maximum resolution of 2.9 Å, were obtained.

As Fig. 1B shows, the overall structure of Stalk shows one dimer in the asymmetric unit, and the structures of the two monomers are similar, with a root-mean-squared deviation (RMSD) of 1.03 Å (Fig. 1D). The Stalk domain of MxB presents as a four-helix bundle, including parallel and anti-parallel helices α1 (residues 418–487), α2 (residues 500–539), α3 (residues 543–579), and α4 (residues 623–669), connected by flexible loops. α4 is followed by a short helix, α5 (residues 672–677), which directs the Stalk domain toward the BSE domain. A 12-aa long loop (L1) divides α1 into α1N and α1C. Loop L2 (amino acids 487–498), connecting α1 and α2, is not visible in the structure. Like MxA, the L4 loop of MxB is highly flexible; thus, the left part of loop L4 (residues 608–618) following the deletion loop is also absent from our model.

3.2. The oligomeric state of the MxB Stalk domain

The Stalk domain of MxB forms an antiparallel dimer, and the dimer interface covers ~1044 Å^2, displaying twofold symmetry between the associating monomers (Fig. 2C). As shown in Fig. 2A, the interface involves residues on helices α3 and α4. Among these residues, M567, L570, M574, V578, F647, and Y651 of each monomer form symmetric hydrophobic contacts with associating residues of the other monomer. These residues that form hydrophobic contacts are located on the edge of the interface. In the center of the interface, it is interesting that eight side chain-mediated hydrogen bonds are formed, as follows: Q571 on each monomer forms two hydrogen bonds with Q644 on the other monomer, and E636 on each monomer forms one hydrogen bond with N643 on the other monomer. Also, R573 on each monomer provides an additional hydrogen bond with Y651. Thus, a large number of hydrogen bonds and hydrophobic contacts contribute to building a stable and compact MxB dimer. With regard to MxA, the dimer interface is stabilized completely by a few intermolecular hydrophobic contacts (Fig. 2B). As compared to the sequence of the Stalk domain of MxA, of all the residues involved in the corresponding dimer interface [28], only L570, M574, V578, and E636 are conserved between MxA and MxB (Fig. 3A), and there is only E636 involved in forming hydrogen bond. These results indicate that although human Mx proteins share common structural characteristics, their dimerization strategies are unique, suggesting that they may have diverse roles in viral restriction.

As previously reported, full-length MxA bearing the YRGR440–443AAAA mutation has lost its oligomerization as well as its dimerization ability, and it presents as a monomer [7]. Our results

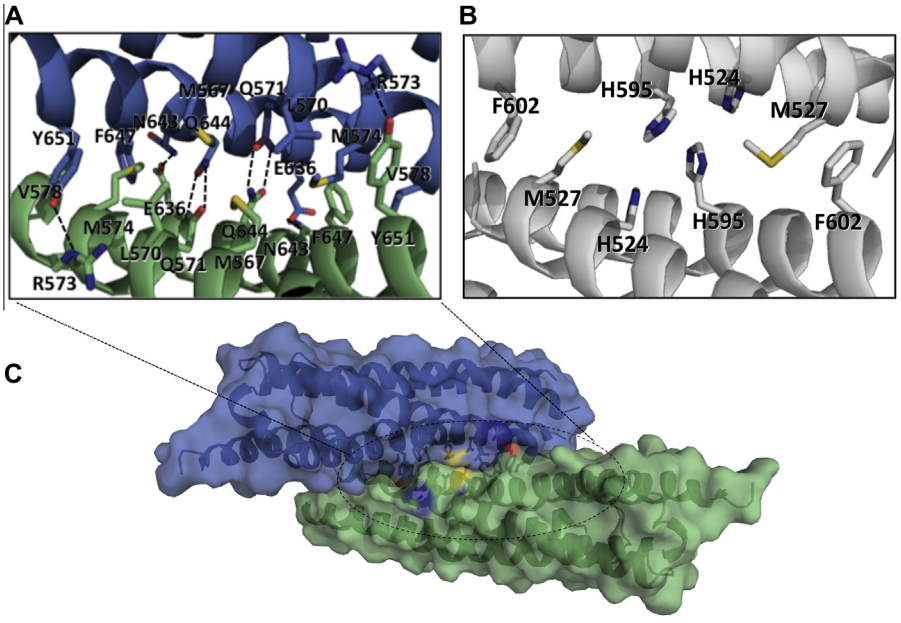

Fig. 2. The dimer interface of human MxB. (A) The dimer interface of the MxB Stalk domain. The hydrogen bonds are indicated by dotted lines, and the residues involved are indicated and shown as sticks. (B) The dimer interface of the MxA Stalk domain. PDB number: 3LJB. The residues involved are shown as sticks. (C) Dimer of MxB Stalk in surface representation.

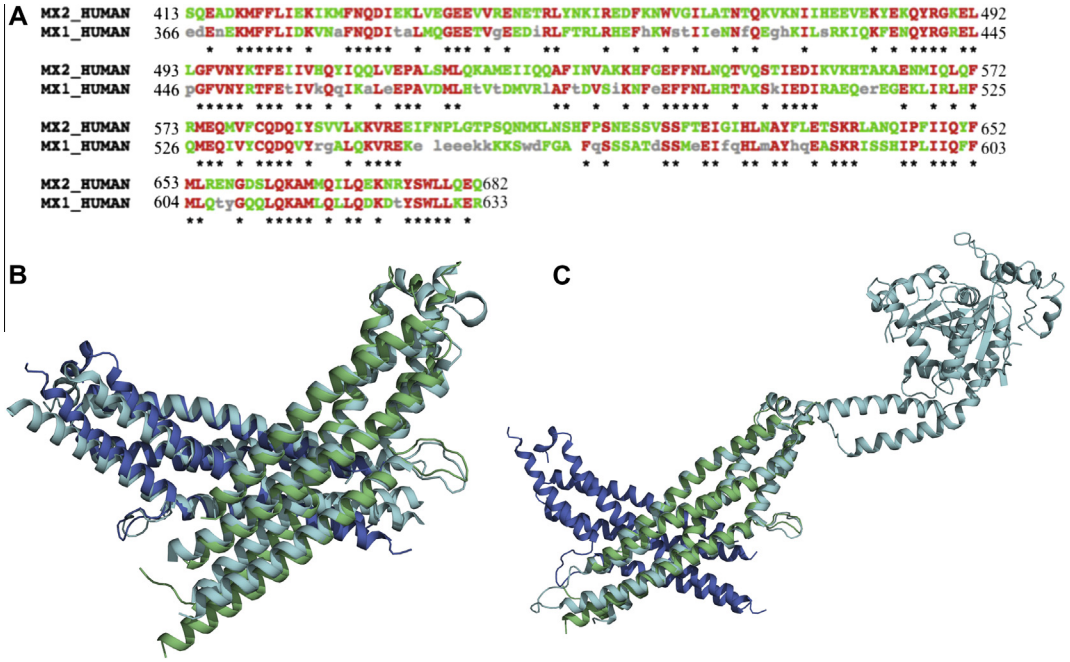

Fig. 3. Alignment of human MxB and MxA. (A) Sequence alignment of the Stalk domains of human MxA and MxB. (B) Structural alignment between the MxB and MxA Stalk domains. (C) Structural alignment between the MxB Stalk domain and full-length MxA. The structures of the MxA Stalk domain (PDB number: 3LJB) and full-length MxA (PDB number: 3SZR) are colored cyan. (For interpretation of the references to color in this figure legend, the reader is referred to the web version of this article.)

show that the MxB Stalk bearing the corresponding YRGK/AAAA mutation maintains the dimerized form in solution (Fig. 1B and C). These results, together with the details of the MxB Stalk dimer interface, suggest that the MxB dimers, not monomers, may be the basic components of the assembly of MxB. Interestingly, we found that MxB Stalk mutants Q571D, R573D, N643D, Q644D, F647D, and Y651D, which are involved in the dimer interface, form inclusion bodies in *E. coli* and become insoluble, indicating that these residues also play critical roles in stabilizing the structure of MxB. Stalk mutants M574D and E636D were partly soluble, but they eluted in the same volume as the wild-type MxB Stalk domain from the size-exclusion column, indicating the stability of MxB dimer (data not shown).

3.3. Structure comparison between human MxB and MxA

MxA and MxB Stalk domains share 46.7% sequence identity (Fig. 3A). In comparison to the structure of the MxA Stalk domain, the overall structure of MxB Stalk presents a similar conformation, as shown is Fig. 3B. The L1 loop of MxB introduces a ~20° kink, which makes its α1C more compact than the α1C of MxA [28]. In comparison to the structure of full-length MxA (Fig. 3C, PDB ID: 3SZR), we found that the conformation and orientation of helix α5, which directs the Stalk domain to the BSE and G domains, are highly conserved. Considering the high sequence identity between MxA and MxB in the G and BSE domains, the overall structure of both Mx proteins is apparently conserved, unlike the corresponding structures of other dynamin-like proteins. This result is consistent with a previous report that a fusion protein combining the N-terminal domain of MxB with the G domain, BSE domain, and Stalk domain of MxA still has antiviral activity. Thus, the structural alignment between MxB Stalk and full-length MxA provides a framework for explaining the molecular details of full-length MxB (Fig. 3C).

In summary, we report the crystal structure of the human MxB Stalk domain and characterization of its assembly properties. Our data establish that Stalk dimerization is a conserved feature of MxB and MxA. However, unique features of MxB's dimerization that differ from those of MxA were also observed. Our structural and biochemical data provide a framework for a mechanistic understanding of the dimerization and assembly of MxB and indicate that the MxB dimer may be the primary form in the assembly and viral restriction of MxB. In the final phase of manuscript preparation, we noted that Fribourgh et al. presented crystal structures of MxB (83–715) [17]. Our crystal structure provides a more detailed picture of the dimer interface of the MxB Stalk domain, which may facilitate further studies of the functional details of MxB's anti-HIV activity.

Acknowledgments

We thank Dr. Yingfang Liu, Dr. Cheng Chen, and Dr. Lizhi Mi for stimulating discussion and Deborah McClellan for editorial assistance. We thank the staff at the BL17U beamline of the SSRF (Shanghai Synchrotron Radiation Facility) in China. This work was supported in part by funding from the Chinese Ministry of Science and Technology (Nos. 2012CB911100 and 2013ZX0001-005) and Tianjin Research Program of Application Foundation and Advanced Technology (No. 14JCQNJC09400).

References

[1] M.A. Horisberger, P. Staeheli, O. Haller, Interferon induces a unique protein in mouse cells bearing a gene for resistance to influenza virus, Proc. Natl. Acad. Sci. U.S.A. 80 (1983) 1910–1914.
[2] H.K. Jin, A. Takada, Y. Kon, O. Haller, T. Watanabe, Identification of the murine Mx2 gene: interferon-induced expression of the Mx2 protein from the feral mouse gene confers resistance to vesicular stomatitis virus, J. Virol. 73 (1999) 4925–4930.
[3] M. Aebi, J. Fah, N. Hurt, C. Samuel, D. Thomis, L. Bazzigher, J. Pavlovic, O. Haller, P. Staeheli, CDNA structures and regulation of two interferon-induced human Mx proteins, Mol. Cell. Biol. 9 (1989) 5062–5072.
[4] G. Kochs, M. Haener, U. Aebi, O. Haller, Self-assembly of human MxA GTPase into highly ordered dynamin-like oligomers, J. Biol. Chem. 277 (2002) 14172–14176.

[5] O. Haller, G. Kochs, Human MxA protein: an interferon-induced dynamin-like GTPase with broad antiviral activity, J. Interferon Cytokine Res. 31 (2011) 79–87.
[6] O. Haller, Dynamins are forever: MxB inhibits HIV-1, Cell Host Microbe 14 (2013) 371–373.
[7] S. Gao, A. von der Malsburg, A. Dick, K. Faelber, Gunnar F. Schröder, O. Haller, G. Kochs, O. Daumke, Structure of myxovirus resistance protein a reveals intra- and intermolecular domain interactions required for the antiviral function, Immunity 35 (2011) 514–525.
[8] J. Lindenmann, Resistance of mice to mouse-adapted influenza A virus, Virology 16 (1962) 203–204.
[9] J. Pavlovic, T. Zurcher, O. Haller, P. Staeheli, Resistance to influenza virus and vesicular stomatitis virus conferred by expression of human MxA protein, J. Virol. 64 (1990) 3370–3375.
[10] E. Gordien, O. Rosmorduc, C. Peltekian, F. Garreau, C. Bréchot, D. Kremsdorf, Inhibition of hepatitis B virus replication by the interferon-inducible MxA protein, J. Virol. 75 (2001) 2684–2691.
[11] K. Melen, P. Keskinen, T. Ronni, T. Sareneva, K. Lounatmaa, I. Julkunen, Human MxB protein, an interferon-alpha-inducible GTPase, contains a nuclear targeting signal and is localized in the heterochromatin region beneath the nuclear envelope, J. Biol. Chem. 271 (1996) 23478–23486.
[12] C. Goujon, O. Moncorge, H. Bauby, T. Doyle, C. Ward, T. Schaller, S. Hue, W. Barclay, R. Schulz, M. Malim, Human MX2 is an interferon-induced post-entry inhibitor of HIV-1 infection, Nature 502 (2013) 559–562.
[13] M. Kane, S. Yadav, J. Bitzegeio, S. Kutluay, T. Zang, S. Wilson, J. Schoggins, C. Rice, M. Yamashita, T. Hatziioannou, P. Bieniasz, MX2 is an interferon-induced inhibitor of HIV-1 infection, Nature 502 (2013) 563–566.
[14] Z. Liu, Q. Pan, S. Ding, J. Qian, F. Xu, J. Zhou, S. Cen, F. Guo, C. Liang, The interferon-inducible MxB protein inhibits HIV-1 infection, Cell Host Microbe 14 (2013) 398–410.
[15] I. Busnadiego, M. Kane, S.J. Rihn, H.F. Preugschas, J. Hughes, D. Blanco-Melo, V.P. Strouvelle, T.M. Zang, B.J. Willett, C. Boutell, P.D. Bieniasz, S.J. Wilson, Host and viral determinants of Mx2 antiretroviral activity, J. Virol. 88 (2014) 7738–7752.
[16] J. Kong, B. Xu, W. Wei, X. Wang, W. Xie, X.F. Yu, Characterization of the amino-terminal domain of Mx2/MxB-dependent interaction with the HIV-1 capsid, Protein Cell (2014).
[17] J.L. Fribourgh, H.C. Nguyen, K.A. Matreyek, F.J. Alvarez, B.J. Summers, T.G. Dewdney, C. Aiken, P. Zhang, A. Engelman, Y. Xiong, Structural insight into HIV-1 restriction by MxB, Cell Host Microbe (2014).
[18] T. Fricke, T. White, B. Schulte, D. de Souza Aranha Vieira, A. Dharan, E. Campbell, A. Brandariz-Nunez, F. Diaz-Griffero, MxB binds to the HIV-1 core and prevents the uncoating process of HIV-1, Retrovirology 11 (2014) 68.
[19] B. Heras, J.L. Martin, Post-crystallization treatments for improving diffraction quality of protein crystals, Acta Crystallogr. D Biol. Crystallogr. 61 (2005) 1173–1180.
[20] Z. Otwinowski, W. Minor, Processing of X-ray diffraction data collected in oscillation mode, in: Methods in Enzymology, vol. 276: Macromolecular Crystallography, Part A, Academic Press, 1997, pp. 307–326.
[21] P.D. Adams, P.V. Afonine, G. Bunkoczi, V.B. Chen, I.W. Davis, N. Echols, J.J. Headd, L.W. Hung, G.J. Kapral, R.W. Grosse-Kunstleve, A.J. McCoy, N.W. Moriarty, R. Oeffner, R.J. Read, D.C. Richardson, J.S. Richardson, T.C. Terwilliger, P.H. Zwart, PHENIX: a comprehensive Python-based system for macromolecular structure solution, Acta Crystallogr. D Biol. Crystallogr. 66 (2010) 213–221.
[22] A.J. McCoy, R.W. Grosse-Kunstleve, P.D. Adams, M.D. Winn, L.C. Storoni, R.J. Read, Phaser crystallographic software, J. Appl. Crystallogr. 40 (2007) 658–674.
[23] T.C. Terwilliger, R.W. Grosse-Kunstleve, P.V. Afonine, N.W. Moriarty, P.H. Zwart, L.W. Hung, R.J. Read, P.D. Adams, Iterative model building, structure refinement and density modification with the PHENIX AutoBuild wizard, Acta Crystallogr. D Biol. Crystallogr. 64 (2008) 61–69.
[24] P. Emsley, K. Cowtan, Coot: model-building tools for molecular graphics, Acta Crystallogr. D Biol. Crystallogr. 60 (2004) 2126–2132.
[25] P.V. Afonine, R.W. Grosse-Kunstleve, N. Echols, J.J. Headd, N.W. Moriarty, M. Mustyakimov, T.C. Terwilliger, A. Urzhumtsev, P.H. Zwart, P.D. Adams, Towards automated crystallographic structure refinement with phenix.refine, Acta Crystallogr. D Biol. Crystallogr. 68 (2012) 352–367.
[26] V.B. Chen, W.B. Arendall 3rd, J.J. Headd, D.A. Keedy, R.M. Immormino, G.J. Kapral, L.W. Murray, J.S. Richardson, D.C. Richardson, MolProbity: all-atom structure validation for macromolecular crystallography, Acta Crystallogr. D Biol. Crystallogr. 66 (2010) 12–21.
[27] M.W. MacArthur, R.A. Laskowski, D.S. Moss, J.M. Thornton, PROCHECK: a program to check the stereochemical quality of protein structures, J. Appl. Crystallogr. 26 (1993) 283–291.
[28] S. Gao, A. Malsburg von der, S. Paeschke, J. Behlke, O. Haller, G. Kochs, O. Daumke, Structural basis of oligomerization in the Stalk region of dynamin-like MxA, Nature 465 (2010) 502–506.